RSC Advances

ROYAL SOCIETY OF CHEMISTRY

www.rsc.org/advances

Title page

Title

Uptake of Nd^{3+} and Sr^{2+} by Li–Al layered double hydroxide intercalated with triethylenetetramine-hexaacetic acid: Kinetic and equilibrium studies

Authors

Tomohito Kameda*, Tetsu Shinmyou, and Toshiaki Yoshioka

Graduate School of Environmental Studies, Tohoku University, 6-6-07 Aoba, Aramaki, Aoba-ku, Sendai 980-8579, Japan.

*Corresponding author:

Tel: +81-22-795-7212; Fax: +81-22-795-7212

E-mail: kameda@env.che.tohoku.ac.jp

Abstract

A Li–Al layered double hydroxide intercalated with triethylenetetramine-hexaacetic acid (TTHA•Li−Al LDH) was prepared by the drop-wise addition of an Al solution to a Li-TTHA solution at a constant pH of 8.0. TTHA•Li−Al LDH was found to take up Nd^{3+} and Sr^{2+} ions from aqueous solutions. This can be attributed to the metal chelating functions of the TTHA species in the interlayer of TTHA•Li−Al LDH, i.e., Nd-TTHA and Sr-TTHA complex were formed in the interlayers. TTHA•Li−Al LDH was found to take up Nd^{3+} ions preferentially over Sr^{2+} ions from aqueous solutions, which can be attributed to the higher stability of the Nd-TTHA complex than Sr-TTHA. The mass-transfer-controlled shrinking core model described the uptake behavior better than the surface reaction-controlled model. The TTHA ions in the TTHA•Li−Al LDH interlayer quickly formed chelate complexes with Nd^{3+} or Sr^{2+}, as a result of which the transfer rate of Nd^{3+} or Sr^{2+} through the product layer was rate limiting. Furthermore, this reaction was suitably represented by the Langmuir-type adsorption mechanism, indicating that it involves chemical adsorption, which is consistent with the formation of chelate complexes between Nd^{3+} or Sr^{2+} and TTHA ions in the interlayers of TTHA•Li−Al LDH.

Introduction

Layered double hydroxides (LDHs) have anion-exchange capabilities and are represented by the general chemical formula $[M^{2+}_{1-x}M^{3+}_{x}(OH)_2](A^{n-})_{x/n}\cdot mH_2O$, where M^{2+} includes Mg^{2+}, Ni^{2+}, and Zn^{2+}; M^{3+} includes $Al^{3+}$and Fe^{3+}; A^{n-} includes CO_3^{2-} and Cl^-; and x represents the molar ratio $M^{3+}/(M^{2+} + M^{3+})$ and assumes values between 0.20 and 0.33 ($0.20 \leqq x \leqq 0.33$).[1-4] While typical LDHs are not capable of taking up cationic metals from aqueous solutions since they have anion-exchange capabilities only, LDHs modified with organic functional groups can take up cationic metals from aqueous solutions.[5] For example, Mg–Al LDHs intercalated with citrate, malate, and tartrate groups have been demonstrated to take up heavy metal ions such as Cu^{2+} and Cd^{2+} ions from aqueous solutions.[6–8] Several researchers have also examined the effect of intercalation of ethylenediaminetetraacetate (EDTA) as a chelating agent in the interlayers of LDHs. Mg–Al, Zn–Al, Cu–Al, and Mg–Fe LDHs intercalated with EDTA are capable of adsorbing metal ions, such as Cu^{2+}, Cd^{2+}, Pb^{2+}, Ni^{2+}, Co^{2+}, Cs^+, Sc^{3+}, Y^{3+}, and La^{3+} in the cationic form from aqueous solutions.[9–18] In our recent study, Zn–Al LDHs intercalated with triethylenetetramine-hexaacetic acid (TTHA•Zn–Al LDH) were prepared by co-precipitation, and their uptake of Nd^{3+} and Sr^{2+} ions from aqueous solutions was investigated.[19] TTHA is an aminocarboxylic acid used as a chelating ligand for metal

ions. TTHA•Zn−Al LDH was found to be superior to EDTA•Zn−Al LDH in its ability to take up Nd^{3+} ions, which can be attributed to the fact that the Nd–TTHA complex is more stable than the Nd–EDTA complex. However, TTHA•Zn−Al LDH was unable to take up Sr^{2+} from aqueous solutions. This was attributed to the intercalation of the Zn-TTHA complex in the interlayers of Zn-Al LDH during the preparation of TTHA•Zn–Al LDH by co-precipitation. Since the Sr-TTHA complex is less stable than the Zn-TTHA complex, Sr^{2+} could not exchange with Zn^{2+} in the Zn-TTHA complex. Furthermore, a large amount of TTHA•Zn–Al LDH was required to obtain a high degree of Nd^{3+} uptake. This was also related to the inability of Nd^{3+} in an aqueous solution to exchange easily with the Zn-TTHA complex intercalated in the interlayer of Zn-Al LDH. Therefore, a key requirement for the uptake of cationic metal ions from aqueous solutions is that the chelate-modified LDH prepared by co-precipitation should not have a metal-chelate complex intercalated in the interlayer.

In this study, a Li–Al LDH intercalated with TTHA (TTHA•Li–Al LDH) was prepared by co-precipitation, and its ability to take up Nd^{3+} and Sr^{2+} ions from aqueous solutions was investigated. Li^{+} is known to form a metal-chelate complex with poor stability.[20] Therefore, Li–Al LDH is expected to have free TTHA ions in the interlayer. In this case, we will explain Li-Al LDH

based on the paper written by Y.-M. Tzou et al.[21] Li-Al LDH has the formula of $[LiAl_2(OH)_6]^+A^-\cdot xH_2O$.[1] Li-Al LDHs are usually synthesized by the incorporation of Li^+ into aluminum hydroxides, i.e., gibbsite or bayerite. In the hydroxide sheets of Li-Al LDH, Li^+ ions are located in the vacant octahedral sites within the gibbsite-like $Al(OH)_3$ layers and contribute to the positively charged sites in the hydroxide layers.[22] In gibbsite, each of the $Al(OH)_3$ layers consists of nearly close packed OH^- ions with Al^{3+} occupying $2/3^{rd}$ of the octahedral holes between alternate layers. The positively charged sites in the hydroxide sheets result from Li^+ ions located in the vacant octahedral holes of the gibbsite-like octahedral Al hydroxide sheet. TTHA•Li–Al LDH is expected to have excellent chelating ability of the TTHA ions in the interlayers and is therefore, expected to take up Nd^{3+} and Sr^{2+} ions from aqueous solutions. Further, to confirm the reaction mechanism, we have conducted kinetic and equilibrium studies on the uptake of Nd^{3+} and Sr^{2+} from aqueous solutions by TTHA•Li−Al LDH.

Experimental

Preparation of NO_3•Li–Al LDH

NO_3•Li–Al LDH was prepared by the drop-wise addition of an Al solution to a Li solution at a constant pH of 8.0. The co-precipitation reaction is expressed by Eq. (1):

$$Li^+ + 2Al^{3+} + NO_3^- + 6OH^- \rightarrow LiAl_2(OH)_6NO_3 \quad (1)$$

The Al solution ($[Al^{3+}]$ = 0.5 mol/L) was prepared by dissolving the required amount of $Al(NO_3)_3$•$9H_2O$ in 250 mL of deionized water, whereas the Li solution ($[Li^+]$ = 2.0 mol/L) was prepared by dissolving the required amount of $LiNO_3$ in 250 mL of deionized water. The Al solution was added drop-wise to the Li solution at a rate of 10 mL/min at 30 °C under mild agitation. The resulting solution was adjusted to pH 8.0 by adding a 1.25 mol/L NaOH solution until the desired pH was achieved. The resulting suspensions were maintained at 30 °C for 1 h at a constant pH of 8.0. The NO_3•Li–Al LDH particles were obtained by filtering the resulting suspension, washing repeatedly with deionized water till neutral pH was achieved, and drying under reduced pressure (133 Pa) at 40 °C for 40 h. N_2 gas was bubbled into the solution throughout the operation to minimize the effect of dissolved CO_2.

Preparation of TTHA•Li–Al LDH

TTHA•Li–Al LDH was prepared by the drop-wise addition of an Al solution to a Li-TTHA ($C_{18}H_{30}N_4O_{12}$) solution at a constant pH of 8.0. At this pH, $C_{18}H_{26}N_4O_{12}^{4-}$ ion is the stable anionic species of TTHA.[23] Therefore, the theoretical formula of TTHA•Li–Al LDH may be given as $LiAl_2(OH)_6(C_{18}H_{26}N_4O_{12})_{0.25}$. The co-precipitation reaction is expressed by Eq. (2).

$$Li^+ + 2Al^{3+} + 0.25C_{18}H_{26}N_4O_{12}^{4-} + 6OH^- \rightarrow LiAl_2(OH)_6(C_{18}H_{26}N_4O_{12})_{0.25} \quad (2)$$

The Al solution ($[Al^{3+}]$ = 0.5 mol/L) was prepared by dissolving the required amount of $Al(NO_3)_3•9H_2O$ in 250 mL of deionized water. Three types of Li-TTHA solutions ($[Li^+]$ = 0.25, 0.5, and 2.0 mol/L; [TTHA] = 0.125 mol/L) were prepared by dissolving the required amounts of $LiOH•H_2O$ and $C_{18}H_{30}N_4O_{12}$ in 250 mL of deionized water. The initial Li/Al molar ratios corresponding to $[Li^+]$ of 0.25, 0.5, and 2.0 mol/L were 0.5, 1.0, and 4.0, respectively. The Al solution was added drop-wise to the Li-TTHA solution at a rate of 10 mL/min at 30 °C under mild agitation. The resulting solution was adjusted to pH 8.0 by the addition of 1.25 mol/L NaOH solution until the desired pH was attained. The resulting suspensions were maintained at 30 °C for 1 h at a constant pH of 8.0. TTHA•Li–Al LDH particles were obtained by filtering the resulting suspension, washing

repeatedly with deionized water until neutral pH was reached, and drying under reduced pressure (133 Pa) at 40 °C for 40 h. N_2 gas was bubbled into the solution throughout the operation to minimize the effect of dissolved CO_2.

Uptake of metal ions from aqueous solutions

The TTHA•Li–Al LDH obtained was added to 500 mL of 1.0 mmol/L $Nd(NO_3)_3$ or $Sr(NO_3)_2$ solution, and the resulting suspensions were maintained at 30 °C for 120 min under stirring at a speed of 300 rpm. N_2 was bubbled into the solutions throughout the experiments. Samples of the suspension were extracted at different time intervals and immediately filtered through a 0.45 μm membrane filter after measuring the pH. The filtrates were then analyzed for Nd^{3+} or Sr^{2+}. The initial molar ratios of TTHA in TTHA•Li–Al LDH to Nd^{3+} and Sr^{2+} ions in the nitrate solutions were set at 1 (i.e., initial TTHA/Nd^{3+} = 1, initial TTHA/Sr^{2+} = 1). Furthermore, the changes in the degrees of Nd^{3+} and Sr^{2+} ion uptake over time using a suspension of TTHA•Li–Al LDH in a 1:1 mixed nitrate solution of Nd^{3+} and Sr^{2+} ions were investigated, when the molar ratio of TTHA in Li–Al LDH to (Nd^{3+} + Sr^{2+}) ions in the mixed nitrate solution was 0.5. To demonstrate the effect

of interlayer anions, NO_3•Li–Al LDH was used as the reference material. The amount of NO_3•Li–Al LDH used was equivalent to that of TTHA•Li−Al LDH.

For the kinetics studies, TTHA•Li−Al LDH was added to 500 mL of 1.0 mmol/L of $Nd(NO_3)_3$ or $Sr(NO_3)_2$ solution, such that the molar ratios of TTHA in TTHA•Li−Al LDH to Nd^{3+} or Sr^{2+} in the nitrate solutions were 1. The resultant suspensions were stirred at 10, 30, or 50 °C for 15 min. N_2 was bubbled into the solutions throughout the experiments. Samples of the suspension were extracted at different time intervals and immediately filtered through a 0.45 μm membrane filter. The filtrates were analyzed for residual Nd^{3+} or Sr^{2+}. For the equilibrium studies, a $Nd(NO_3)_3$ or $Sr(NO_3)_2$ solution (20 mL of 2–7 mmol/L solution) and 0.1 g of TTHA•Li−Al LDH were placed in a 50 mL screw-top tube and shaken at 30 °C for 7 d. Samples of the suspension were filtered through a 0.45 μm membrane filter and the filtrates were analyzed for Nd^{3+} or Sr^{2+}.

Characterization methods

NO_3•Li–Al LDH, TTHA•Li–Al LDH, and TTHA•Li–Al LDH loaded with Nd^{3+} and Sr^{2+} ions were analyzed by X-ray diffraction (XRD) using CuKα radiation. The particle morphologies of NO_3•Li–Al LDH and TTHA•Li–Al LDH

were observed by scanning electron micrography (SEM). The average particle size and ζ-potentials of NO_3•Li–Al LDH and TTHA•Li–Al LDH were analyzed by dynamic light scattering. The Li^+ and Al^{3+} ions in the solutions were determined by inductively coupled plasma-atomic emission spectrometry (ICP-AES) by dissolving the LDHs in 1 mol/L HNO_3. The materials were dissolved in 1 mol/L HNO_3 and analyzed for TTHA based on the total organic carbon (TOC) content. For the adsorption experiments, the residual concentrations of Nd^{3+} and Sr^{2+} ions in the filtrates were determined by ICP-AES.

Results and Discussion

Preparation

Fig. 1 shows the XRD patterns of (a) NO_3•Li−Al LDH and TTHA•Li−Al LDHs prepared with initial Li/Al molar ratios of (b) 0.5, (c) 1.0, and (d) 4.0. The XRD peaks observed for NO_3•Li−Al LDH (Fig. 1a) were attributed to lithium aluminum nitrate hydroxide hydrate (JCPDS card No. 51-359) formulated as $LiAl_2(OH)_6NO_3$•xH_2O with an LDH structure, whereas the XRD peaks were also attributed to $Al(OH)_3$ (JCPDS card No. 12-460). The presence of $Al(OH)_3$ in Li-Al

LDH was also observed in previous studies.[21,24] For NO_3•Li−Al LDH, the observed basal spacing, d_{003}, was 9.0 Å, with an LDH host layer thickness of 4.8 Å and an interlayer spacing of 4.2 Å. On the other hand, the XRD pattern of the TTHA•Li−Al LDHs (Figs. 1b–d) did not exhibit peaks corresponding to $Al(OH)_3$. The peaks for this material were also broader than those for NO_3•Li–Al LDH (Fig. 1a). However, the similarities in the other peak locations observed in the XRD patterns of both the materials indicate that the TTHA•Li−Al LDHs have a LDH structure. The intercalation of TTHA ions, which are larger than NO_3^- ions, in the interlayer of Li–Al LDH, is confirmed by the increase in the basal spacing from 9.0 Å to ~16 Å. The peak intensity of the basal spacing increased with increase in the initial Li/Al molar ratio. This is attributed to the increase in the amount of Li^+ incorporated in the vacancy of the $Al(OH)_3$ host lattice in Li-Al LDH. In other words, the increase in the peak intensity corresponds to an increase in the crystallinity of the LDH. As shown in Fig. 1d, TTHA•Li−Al LDH prepared with an initial Li/Al molar ratio of 4.0 exhibited the highest crystallinity among all the samples with various Li/Al molar ratios. Fig. 1d shows that the TTHA•Li–Al LDH sample with an initial Li/Al molar ratio of 4.0 has a basal spacing of 14.3 Å with an interlayer spacing of 9.5 Å. The length of TTHA was previously calculated to be

12.1 Å,[19] which is larger than the above-mentioned interlayer spacing. Therefore, the TTHA ion was most likely inclined at 54.1° with respect to the $Al(OH)_3$ host layers in Li-Al LDH. Table 1 shows the chemical compositions of NO_3•Li−Al LDH and TTHA•Li−Al LDHs prepared at initial Li/Al molar ratios of 0.5, 1.0, and 4.0. The theoretical Li/Al molar ratio for these LDHs calculated based on Eqs. (1–2) is 0.5. The actual Li/Al molar ratio was 0.3 for NO_3•Li−Al LDH, and the TTHA•Li−Al LDHs prepared at initial Li/Al molar ratios of 0.5 and 1.0. It may be noted that the actual Li/Al molar ratio was lower than the theoretical Li/Al molar ratio, which suggests that the Li^+ and Al^{3+} ions in the solutions precipitated as Li−Al LDH. In the case of TTHA•Li−Al LDH, the actual Li/Al molar ratio was 0.7 for the sample prepared at an initial Li/Al molar ratio of 4.0. In other words, the actual Li/Al molar ratio was larger than the theoretical Li/Al molar ratio of 0.5, which implies that a small amount of Li^+ was combined with TTHA in the aqueous solution, in addition to the precipitation of the large amount of Li^+ as Li-Al LDH. The complex of Li^+ and TTHA (i.e. $[Li\text{-}C_{18}H_{26}N_4O_{12}]^{3-}$) was intercalated in the interlayers of Li-Al LDH. For the TTHA•Li−Al LDHs, the actual TTHA/Li molar ratios were in the range of 0.14–0.33, whereas the theoretical TTHA/Li molar ratio, as indicated by Eq. (2), is 0.25. The actual TTHA/Li molar ratio for the sample

with the initial Li/Al molar ratio of 4.0 was lower than the theoretical value of 0.25, indicating that the $C_{18}H_{26}N_4O_{12}^{4-}$ and $[Li\text{-}C_{18}H_{26}N_4O_{12}]^{3-}$ complexes were intercalated in the Li–Al LDH interlayer. In contrast, the actual TTHA/Li molar ratios for the samples with the initial Li/Al molar ratios of 0.5 and 1.0 were larger than the theoretical value of 0.25, indicating that $C_{18}H_{26}N_4O_{12}^{4-}$ was intercalated in the Li–Al LDH interlayer, and $C_{18}H_{26}N_4O_{12}^{4-}$ was probably adsorbed on the surface of Li–Al LDH. Fig. 2 shows the SEM images of (a) NO_3•Li−Al LDH and (b) TTHA•Li−Al LDH, both prepared at initial Li/Al molar ratios of 4.0. In both the cases, the crystals exhibit a plate-like morphology, which is similar to the crystal structure of Li-Al LDH.[25] Table 2 shows the average particle size and ζ-potentials of NO_3•Li−Al and TTHA•Li−Al LDH prepared at initial Li/Al molar ratios of 4.0. The average particle size of TTHA•Li−Al LDH was found to be larger than that of NO_3•Li−Al LDH. In addition, the surfaces of TTHA•Li−Al LDH and NO_3•Li−Al LDH were found to be positively charged.

In summary, NO_3•Li−Al LDH and TTHA•Li−Al LDH were prepared by the co-precipitation method. As shown in Fig. 1d, TTHA•Li−Al LDH samples prepared with an initial Li/Al molar ratio of 4.0 exhibited the highest crystallinity among all the samples prepared at various initial Li/Al molar ratios. Therefore,

TTHA•Li−Al LDH prepared with the initial Li/Al molar ratio of 4.0 was used to study the uptake of metal ions from aqueous solutions. Hereafter, TTHA•Li-Al LDH refers to the sample prepared with an initial Li/Al molar ratio of 4.0.

Uptake of metal ions from aqueous solutions

Fig. 3 shows the variation in Nd^{3+} or Sr^{2+} uptake over time during the suspension of TTHA•Li−Al LDH or NO_3•Li−Al LDH in $Nd(NO_3)_3$ and $Sr(NO_3)_2$ solutions. The amounts of Nd^{3+} and Sr^{2+} uptake by TTHA•Li−Al LDH increased with time. The Nd^{3+} uptake behavior was almost similar to that of Sr^{2+}. In other words, little difference was observed in the Nd^{3+} and Sr^{2+} uptake behaviors of TTHA•Li−Al LDH. In contrast, Nd^{3+} and Sr^{2+} uptake were below 20% for NO_3•Li–Al LDH during all the sampling times. This difference in the Nd^{3+} and Sr^{2+} uptake between TTHA•Li−Al LDH and NO_3•Li−Al LDH can be attributed to the role of the $C_{18}H_{26}N_4O_{12}^{4-}$ ion and the $[Li\text{-}C_{18}H_{26}N_4O_{12}]^{3-}$ complex in the interlayer of TTHA•Li−Al LDH. $[Nd\text{-}C_{18}H_{26}N_4O_{12}]^{-}$ or $[Sr\text{-}C_{18}H_{26}N_4O_{12}]^{2-}$ complexes were formed in the interlayers of TTHA•Li−Al LDH, as a result of

interactions between Nd^{3+} or Sr^{2+} and the $C_{18}H_{26}N_4O_{12}{}^{4-}$ ion, as shown in Eqs. (3-4).

$$Nd^{3+} + C_{18}H_{26}N_4O_{12}{}^{4-} \rightleftarrows [Nd\text{-}C_{18}H_{26}N_4O_{12}]^{-} \quad (3)$$

$$Sr^{2+} + C_{18}H_{26}N_4O_{12}{}^{4-} \rightleftarrows [Sr\text{-}C_{18}H_{26}N_4O_{12}]^{2-} \quad (4)$$

Similarly, $[Nd\text{-}C_{18}H_{26}N_4O_{12}]^{-}$ or $[Sr\text{-}C_{18}H_{26}N_4O_{12}]^{2-}$ complexes were most likely formed in the interlayers of TTHA•Li−Al LDH as a result of interactions between Nd^{3+} or Sr^{2+} and $[Li\text{-}C_{18}H_{26}N_4O_{12}]^{3-}$, as indicated in Eqs. (5-6).

$$Nd^{3+} + [Li\text{-}C_{18}H_{26}N_4O_{12}]^{3-} \rightleftarrows [Nd\text{-}C_{18}H_{26}N_4O_{12}]^{-} + Li^{+} \quad (5)$$

$$Sr^{2+} + [Li\text{-}C_{18}H_{26}N_4O_{12}]^{3-} \rightleftarrows [Sr\text{-}C_{18}H_{26}N_4O_{12}]^{2-} + Li^{+} \quad (6)$$

This behavior may be caused by the difference in the stabilities of the $[Nd\text{-}C_{18}H_{26}N_4O_{12}]^{-}$ or $[Sr\text{-}C_{18}H_{26}N_4O_{12}]^{2-}$ complexes and the $[Li\text{-}C_{18}H_{26}N_4O_{12}]^{3-}$ complex. It may be noted that the metal-chelate formation constants for TTHA and Nd^{3+} or Sr^{2+} were 22.8 or 9.3, respectively,[26,27] whereas the metal-chelate formation constant for TTHA and Li^{+} was determined to be 3.6 by our analysis according to a previous method.[26,27] Thus, the $[Nd\text{-}C_{18}H_{26}N_4O_{12}]^{-}$ or $[Sr\text{-}C_{18}H_{26}N_4O_{12}]^{2-}$ complexes were much more stable than the $[Li\text{-}C_{18}H_{26}N_4O_{12}]^{3-}$ complex. Therefore, the reaction shown in Eqs. (5-6) is considered to have occurred easily.

Fig. 3 also shows that the Nd^{3+} ion uptake by NO_3•Li–Al LDH was 16.1% after 120 min, probably due to the precipitation of Nd^{3+} ions as $Nd(OH)_3$ caused by the increase in pH resulting from the addition of LDH. In fact, the pH of NO_3•Li–Al LDH vs. Nd^{3+} increased rapidly from 5.5 to 6.5 in a short time, following which it remained constant (Fig. 4). This can be attributed to the buffer action exhibited by the Al^{3+} dissolved from Li–Al LDH. In particular, a larger pH increase was prevented by the buffer action resulting in less precipitation of Nd^{3+} ions as $Nd(OH)_3$. Notably, TTHA•Li−Al LDH was able to take up almost all the Nd^{3+} ions from the solutions in the cationic form. Fig. 3 also shows that the Sr^{2+} ion uptake for NO_3•Li–Al LDH was 6.4% after 120 min. As shown in Fig. 4, the pH of NO_3•Li–Al LDH vs. Sr^{2+} increased from 5.8 to 7.7 in 120 min. This can also be attributed to the buffer action of the Al^{3+} dissolved from Li–Al LDH. However, Sr^{2+} ion was barely precipitated as hydroxide. On the other hand, we reported previously that $Al(OH)_3$ could take up Sr^{2+}.[19] The uptake of Sr^{2+} ions by $Al(OH)_3$ can be attributed to the co-precipitation of Al hydrolysate (i.e., $Al(OH)_2^+$ and $Al(OH)^{2+}$) and Sr^{2+} ions. Therefore, the Sr^{2+} ion uptake by NO_3•Li−Al LDH can be attributed to the co-precipitation of Sr^{2+} ions and Al hydrolysate derived from LDH. After all, the Sr^{2+} ion uptake by NO_3•Li−Al LDH was much lower than that

by TTHA•Li−Al LDH. It may be noted that TTHA•Li−Al LDH could take up almost all the Sr^{2+} ions from the solutions in the cationic form.

In our previous paper, we examined the ability of TTHA•Zn−Al LDH to take up Nd^{3+} and Sr^{2+} from aqueous solutions.[19] TTHA•Zn−Al LDH was found to adsorb Nd^{3+} ions from aqueous solutions, with an Nd^{3+} uptake of 91.5% at an initial TTHA/Nd^{3+} molar ratio of 5 in 120 min. On the other hand, TTHA•Zn−Al LDH could barely take up Sr^{2+} from aqueous solutions, which was attributed to the presence of the Zn-TTHA complex intercalated in the interlayers of Zn-Al LDH. Since the stability of the Sr-TTHA complex is lower than that of the Zn-TTHA complex, Sr^{2+} could not exchange with Zn^{2+} in the Zn-TTHA complex. Furthermore, an initial TTHA/Nd^{3+} molar ratio of 5 was required in order to obtain a high degree of Nd^{3+} uptake. This is also caused by the formation of the Zn-TTHA complex intercalated in the interlayers of Zn-Al LDH, which cannot be easily exchanged with Nd^{3+} from an aqueous solution. In contrast, it must be noted that TTHA•Li−Al LDH could take up Nd^{3+} and Sr^{2+} easily from aqueous solutions at initial TTHA/Nd^{3+} or Sr^{2+} molar ratios of 1, as shown in Fig. 3. This suggests that TTHA•Li−Al LDH contained a large amount of $C_{18}H_{26}N_4O_{12}^{4-}$ ions, i.e., free TTHA ions, in the interlayers, leading to the facile formation of

$[Nd\text{-}C_{18}H_{26}N_4O_{12}]^-$ or $[Sr\text{-}C_{18}H_{26}N_4O_{12}]^{2-}$ complexes in the interlayers during the uptake of Nd^{3+} and Sr^{2+}, respectively. The facile uptake of Nd^{3+} and Sr^{2+} by TTHA•Li−Al LDH may also be caused by the intercalation of the Li-TTHA complex in the interlayers of Li-Al LDH, which is easily exchanged with Nd^{3+} and Sr^{2+} in aqueous solutions.

Fig. 5 shows the XRD patterns for products obtained from the suspension of TTHA•Li−Al LDH in the (a) $Nd(NO_3)_3$ and (b) $Sr(NO_3)_2$ solutions in 120 min. Compared to the original XRD patterns of TTHA•Li−Al LDH (Fig. 1d), few detectable shifts in the positions of the diffraction peaks were observed for peaks corresponding to the basal spacing. This indicates that the uptake of Nd^{3+} or Sr^{2+} did not disrupt the interlayer spacing, indicating that the $[Nd\text{-}C_{18}H_{26}N_4O_{12}]^-$ or $[Sr\text{-}C_{18}H_{26}N_4O_{12}]^{2-}$ complex was easily formed in the interlayers of TTHA•Li−Al LDH.

Fig. 6 shows the variations in Nd^{3+} and Sr^{2+} uptake with time during the suspension of TTHA•Li−Al LDH in 1:1 mixed nitrate solution of Nd^{3+} and Sr^{2+}. The degree of Nd^{3+} ion uptake increased rapidly during the initial stages, following which it increased gradually over time. On the other hand, the degree of Sr^{2+} ion uptake increased rapidly with time during the initial stages, and was then almost

constant beyond a certain duration of time. It may be noted that the degree of uptake of Nd^{3+} was greater than that of Sr^{2+} for all the sampling times and in 120 min, the degrees of Nd^{3+} and Sr^{2+} ion uptake were 79.0% and 19.0%, respectively. In other words, the degree of selectivity, i.e., the ratio of Nd^{3+}/Sr^{2+} uptake was 4.2. TTHA•Li−Al LDH was found to take up Nd^{3+} ions preferentially over Sr^{2+} ions from solutions, which can be attributed to the difference in the stabilities of the $[Nd\text{-}C_{18}H_{26}N_4O_{12}]^-$ and $[Sr\text{-}C_{18}H_{26}N_4O_{12}]^{2-}$ complexes. The metal-chelate formation constants for the Nd-TTHA and Sr-TTHA complexes have been reported to be 22.8 and 9.3, respectively.[26,27] In other words, the $[Nd\text{-}C_{18}H_{26}N_4O_{12}]^-$ complex was more stable than the $[Sr\text{-}C_{18}H_{26}N_4O_{12}]^{2-}$ complex. Nd^{3+} ions easily form the $[Nd\text{-}C_{18}H_{26}N_4O_{12}]^-$ complex with the $C_{18}H_{26}N_4O_{12}^{4-}$ ions in the interlayers of TTHA•Li−Al LDH, and easily exchange with the Li^+ ions in the $[Li\text{-}C_{18}H_{26}N_4O_{12}]^{3-}$ complex present in the interlayer. In contrast, the $[Sr\text{-}C_{18}H_{26}N_4O_{12}]^{2-}$ complex is difficult to form from the Sr^{2+} and $C_{18}H_{26}N_4O_{12}^{4-}$ ions in the interlayers of TTHA•Li−Al LDH, owing to the poor stability of $[Sr\text{-}C_{18}H_{26}N_4O_{12}]^{2-}$ compared to $[Nd\text{-}C_{18}H_{26}N_4O_{12}]^-$.

Fig. 7 shows the effect of temperature on the degree of Nd^{3+} uptake by a suspension of TTHA•Li−Al LDH in the $Nd(NO_3)_3$ solution. The uptake initially

increased sharply, following which it continued to increase more gradually at longer times. At over 2 min, the uptake was observed to increase slightly with increase in temperature. Fig. 8 also shows the effect of temperature on the degree of Sr^{2+} uptake by the suspension of TTHA•Li−Al LDH in $Sr(NO_3)_2$ solution. Similar to the Nd^{3+} uptake behavior, Sr^{2+} uptake increased sharply during the initial stages, following which it continued to increase gradually at longer times. At over 4 min, the Sr^{2+} uptake was observed to increase slightly with increase in temperature. To understand whether the reaction proceeds under surface chemical reaction control or mass transfer control, the experimental data were arranged according to the shrinking core model, in which the TTHA•Li−Al LDH particles are approximated as spheres.[28,29] In the case of surface chemical reaction control, the relationship between time and the degree of Nd^{3+} or Sr^{2+} uptake can be expressed as

$$1 - (1 - x)^{1/3} = kt, \qquad (7)$$

where x is the degree of Nd^{3+} or Sr^{2+} uptake and k (/min) is the apparent rate constant. If, however, the rate of transfer of Nd^{3+} or Sr^{2+} through the product layer is rate-limiting, i.e., the uptake is mass transfer controlled, then the following equation may apply (Eq. (8)):

$$1 - 3(1 - x)^{2/3} + 2(1 - x) = kt. \qquad (8)$$

Fig. 9 shows the experimental data for the uptake of Nd^{3+} by TTHA•Li-Al LDH plotted according to Eq. (7). The plots show good linearity at all the temperatures. Further, the value of the intercept was non-zero at all the temperatures, suggesting that the precipitation of Nd^{3+} as $Nd(OH)_3$ occurred rapidly.[19] The apparent rate constants (k) at 10, 30, and 50 °C, determined from the slopes of the straight lines in Fig. 9, were 8.5×10^{-3}, 9.1×10^{-3}, and 1.1×10^{-2} min^{-1}, respectively. Fig. 10 shows the experimental data for the uptake of Sr^{2+} by TTHA•Li-Al LDH plotted according to Eq. (7). The plots show good linearity at all the temperatures. Similar to the case of Nd^{3+}, the values of the intercepts were non-zero at all the temperatures, suggesting that the co-precipitation of Sr^{2+} with the Al hydrolysate derived from LDH occurred rapidly.[19] The apparent rate constants (k) at 10, 30, and 50 °C, determined from the slopes of the straight lines in Fig. 10, were 6.6×10^{-3}, 7.6×10^{-3}, and 5.8×10^{-3} min^{-1}, respectively. An Arrhenius plot of these k values is shown in Fig. 11. This plot does not deviate significantly from linearity, indicating that the reaction does not proceed under surface chemical reaction control. Fig. 12 shows the experimental data for the uptake of Nd^{3+} by TTHA•Li-Al LDH, plotted according to Eq. (8). The plots for each temperature show good linearity. Further, the apparent rate constants (k) at 10, 30, and 50 °C, determined from the slopes of the straight lines in Fig. 12, were 9.3×10^{-3}, 1.2×10^{-3}, and 1.6×10^{-2} min^{-1}, respectively. Fig. 13

presents the experimental data for the uptake of Sr^{2+} by TTHA•Li-Al LDH plotted according to Eq. (8). The plots for each temperature show good linearity in this case also. The apparent rate constants (k) at 10, 30, and 50 °C, determined from the slopes of the straight lines in Fig. 13, were 8.5×10^{-5}, 9.1×10^{-4}, and 9.5×10^{-4} min^{-1}, respectively. An Arrhenius plot for the uptake of Nd^{3+} and Sr^{2+} by TTHA•Li-Al LDH is shown in Fig. 14. In the cases of both Nd^{3+} and Sr^{2+}, the plots are linear. Further, apparent activation energies of 9.8 and 2.1 kJ/mol are calculated for Nd^{3+} and Sr^{2+}, respectively. These values are consistent with the apparent activation energy expected under mass transfer control, which is below 40 kJ/mol.[30] This result confirms that the reaction involved in the uptake of Nd^{3+} and Sr^{2+} by TTHA•Li−Al LDH proceeds under mass transfer control. Further, this suggests that the TTHA ions in the interlayers of TTHA•Li−Al LDH rapidly form chelate complexes with Nd^{3+} and Sr^{2+}. Therefore, the transfer of Nd^{3+} and Sr^{2+} through the product layer is rate-limiting.

Fig. 15 shows the adsorption isotherms of Nd^{3+} and Sr^{2+} adsorbed by TTHA•Li−Al LDH. The equilibrium adsorption amounts increased with increase in the equilibrium concentration in both the cases. In both the cases, the isotherm curves shown in Fig. 15 are considered to represent Langmuir-type

adsorption, as confirmed by arranging the experimental data according to the Langmuir equation, which can be expressed as

$$q_e = C_e q_m K_L/(1 + C_e K_L), \quad (9)$$

where q_e (mmol/g) is the equilibrium adsorption amount, C_e (mmol/L) is the equilibrium concentration, q_m (mmol/g) is the maximum adsorption amount, and K_L is the equilibrium adsorption constant. Eq. (9) may be rearranged into the form shown in Eq. (10):

$$C_e/q_e = 1/q_m K_L + C_e/q_m. \quad (10)$$

Fig. 16 shows the experimental adsorption isotherm data for the adsorption of Nd^{3+} and Sr^{2+} on TTHA•Li−Al LDH, plotted according to Eq. (10). In both the cases, the plots exhibit good linearity, indicating that the adsorption can be expressed by a Langmuir-type mechanism. This indicates that the reaction involves monolayer adsorption, i.e., chemical adsorption, suggesting the formation of chelate complexes between Nd^{3+} or Sr^{2+} and TTHA ions in the interlayers of TTHA•Li−Al LDH. In the case of Nd^{3+}, the value of K_L, determined from the slope and intercept of the straight line in Fig. 16, was 19.8, whereas the value of q_m was 0.6 mmol/g. For Sr^{2+}, the value of K_L was 8.1, whereas the value of q_m was 0.5 mmol/g.

Conclusions

TTHA•Li–Al LDH was prepared by the drop-wise addition of Al solution to a Li-TTHA ($C_{18}H_{30}N_4O_{12}$) solution at a constant pH of 8.0. The as-synthesized TTHA•Li−Al LDH contained the $C_{18}H_{26}N_4O_{12}^{4-}$ ion and $[Li\text{-}C_{18}H_{26}N_4O_{12}]^{3-}$ complex in its interlayers. TTHA•Li−Al LDH was found to take up Nd^{3+} and Sr^{2+} ions from aqueous solutions, which can be attributed to the metal-chelating functions of the $C_{18}H_{26}N_4O_{12}^{4-}$ and $[Li\text{-}C_{18}H_{26}N_4O_{12}]^{3-}$ species in the interlayers of the TTHA•Li−Al LDH. In other words, $[Nd\text{-}C_{18}H_{26}N_4O_{12}]^{-}$ and $[Sr\text{-}C_{18}H_{26}N_4O_{12}]^{2-}$ complex could be formed in the interlayers, owing to the higher stability of the $[Nd\text{-}C_{18}H_{26}N_4O_{12}]^{-}$ and $[Sr\text{-}C_{18}H_{26}N_4O_{12}]^{2-}$ complexes compared to the $[Li\text{-}C_{18}H_{26}N_4O_{12}]^{3-}$ complex. Further, TTHA•Li−Al LDH was found to take up Nd^{3+} ions preferentially over Sr^{2+} ions from aqueous solutions, which can be attributed to the higher stability of $[Nd\text{-}C_{18}H_{26}N_4O_{12}]^{-}$ compared to $[Sr\text{-}C_{18}H_{26}N_4O_{12}]^{2-}$. The mass-transfer-controlled shrinking core model described the uptake behavior better than the surface reaction-control model. The TTHA ions in the TTHA•Li−Al LDH interlayer rapidly form chelate complexes with Nd^{3+} or Sr^{2+}, as a result of which the transfer of Nd^{3+} or Sr^{2+} through the product layer is rate limiting. Furthermore, this reaction can be expressed by a Langmuir-type adsorption mechanism, indicating that this reaction involves chemical adsorption,

consistent with the formation of chelate complexes between Nd^{3+} or Sr^{2+} and TTHA ions in the interlayers of TTHA•Li−Al LDH.

Notes and references

1 F. Cavani, F. Trifirò, A. Vaccari, *Catal. Today,* 1991, **11**, 173.

2 L. Ingram, H.F.W. Taylor, *Mineral. Mag.,* 1967, **36**, 465.

3 R. Allmann, *Acta Crystallogr.*, 1968, **B24**, 972.

4 S.J. Mills, A.G. Christy, J.-M.R. Génin, T. Kameda, F. Colombo, *Mineral. Mag.*, 2012, **76**, 1289.

5 J. Cuppoletti (Ed.), Metal, ceramic and polymeric composites for various uses, InTech, Croatia, 2011.

6 T. Kameda, H. Takeuchi, T. Yoshioka, *Sep. Purif. Technol*., 2008, **62**, 330.

7 T. Kameda, H. Takeuchi, T. Yoshioka, *Mater. Res. Bull*., 2009, **44**, 840.

8 T. Kameda, H. Takeuchi, T. Yoshioka, *Colloids Surf. A: Physicochem. Eng. Aspects*, 2010, **355**, 172.

9 T. Kameda, S. Saito, Y. Umetsu, *Sep. Purif. Technol*., 2005, **47**, 20.

10 M. R. Perez, I. Pavlovic, C. Barriga, J. Cornejo, M. C. Hermosin, M. A. Ulibarri, *Appl. Clay Sci*., 2006, **32**, 245.

11 R. Rojas, M. R. Perez, E. M. Erro, P. I. Ortiz, M. A. Ulibarri, C. E. Giacomelli, *J. Colloid Interf. Sci*., 2009, **331**, 425.

12 S. A. Kulyukhin, E. P. Krasavina, I. V. Gredina, I. A. Rumer, L. V. Mizina, *Radiochemistry*, **2008**, *50*, 493.

13 S. R. J. Oliver, *Chem. Soc. Rev*., 2009, **38**, 1868.

14 V. V. Goncharuk, L. N. Puzyrnaya, G. N. Pshinko, A. A. Kosorukov, V. Y. Demchenko, *J. Wat. Chem. Tech*., 2011, **33**, 288.

15 S. A. Kulyukhin, E. P. Krasavina, I. A. Rumer, L. V. Mizina, N. A. Konovalova, I. V. Gredina, *Radiochemistry*, 2011, **53**, 504.

16 T. Kameda, K. Hoshi, T. Yoshioka, *Solid State Sci*., 2011, **13**, 366.

17 T. Kameda, K. Hoshi, T. Yoshioka, *Mater. Res. Bull*., 2012, **47**, 4216.

18 T. Kameda, K. Hoshi, T. Yoshioka, *Solid State Sci*., 2013, **17**, 28.

19 T. Kameda, T. Shimmyo, T. Yoshioka, *RSC Adv.*, 2014, **4**, 45995.

20 R. M. Smith, A. E. Martell, Critical Stability Constants. Plenum Press, New York, 1989.

21 Y.-M. Tzou, S.-L. Wang, L.-C. Hsu, R.-R. Chang, C. Lin, *Appl. Clay Sci.*, 2007, **37**, 107.

22 V. Besserguenev, A. M. Fogg, R. J. Francis, S. J. Price, D. O'Hare, V. P. Isupov, B. P. Tolochko, *Chem. Mater.*, 1997, **9**, 241.

23 P. Letkeman, A. E. Martell, *Inorg. Chem*., 1979, **18**, 1284.

24 L. C. Hsu, S. L. Wang, Y. M. Tzou, C. F. Lin, J. H. Chen, *J. Hazard. Mater.*, 2007, **142**,

242.

25 S.-L. Wang, C.-H. Lin, Y.-Y. Yan, M. K. Wang, *Appl. Clay Sci.*, 2013, **72**, 191.

26 L. Harju, A. Ringbom, *Anal. Chim. Acta*, 1970, **49**, 221.

27 L. Harju, *Anal. Chim. Acta*, 1970, **50**, 475.

28 T. Sato, M. Tezuka, T. Endo, M. Shimada, *React. Solids*, 1987, **3**, 287.

29 T. Kameda, T. Yoshioka, T. Hoshi, M. Uchida, A. Okuwaki, *Sep. Purif. Technol.*, 2006, **51**, 272.

30 Nihon Bunseki Kagakukai, Hokkaidou Sibu•Touhoku Sibu. Bunseki Kagaku Hannou no Kiso, Baifuukan, Japan, 1994.

Figure captions

Fig. 1 XRD patterns of (a) NO_3•Li−Al LDH and TTHA•Li−Al LDHs prepared at initial Li/Al molar ratios of (b) 0.5, (c) 1.0, and (d) 4.0.

Fig. 2 SEM images of (a) NO_3•Li−Al LDH and (b) TTHA•Li−Al LDH prepared at initial Li/Al molar ratios of 4.0.

Fig. 3 Variation in Nd^{3+} or Sr^{2+} uptake over time during the suspension of TTHA•Li−Al LDH or NO_3•Li−Al LDH in $Nd(NO_3)_3$ or $Sr(NO_3)_2$ solutions.

Fig. 4 Variation in pH after Nd^{3+} or Sr^{2+} uptake with time during the suspension of TTHA•Li−Al LDH or NO_3•Li−Al LDH in $Nd(NO_3)_3$ or $Sr(NO_3)_2$ solutions.

Fig. 5 XRD patterns of the products obtained from the suspension of TTHA•Li−Al LDH in (a) $Nd(NO_3)_3$ and (b) $Sr(NO_3)_2$ solutions in 120 min.

Fig. 6 Variations in Nd^{3+} and Sr^{2+} uptake with time during the suspension of

TTHA•Li−Al LDH in 1:1 mixed nitrate solution of Nd^{3+} and Sr^{2+}.

Fig. 7 Effect of temperature on the degree of Nd^{3+} uptake by the suspension of TTHA•Li-Al LDH in $Nd(NO_3)_3$ solution.

Fig. 8 Effect of temperature on the degree of Sr^{2+} uptake by the suspension of TTHA•Li-Al LDH in $Sr(NO_3)_2$ solution.

Fig. 9 Experimental data for the uptake of Nd^{3+} by TTHA•Li-Al LDH, plotted according to the equation describing surface chemical reaction control (Eq. (7)).

Fig. 10 Experimental data for the uptake of Sr^{2+} by TTHA•Li-Al LDH, plotted according to the equation describing surface chemical reaction control (Eq. (7)).

Fig. 11 Arrhenius plot of the apparent rate constants for surface chemical reaction control during the uptake of Nd^{3+} and Sr^{2+} by TTHA•Li-Al LDH.

Fig. 12 Experimental data for the uptake of Nd^{3+} by TTHA•Li-Al LDH, plotted according

to the equation describing mass transfer control (Eq. (8)).

Fig. 13 Experimental data for the uptake of Sr^{2+} by TTHA•Li-Al LDH, plotted according to the equation describing mass transfer control (Eq. (8)).

Fig. 14 Arrhenius plot of the apparent rate constants for mass transfer control during the uptake of Nd^{3+} and Sr^{2+} by TTHA•Li-Al LDH.

Fig. 15 Adsorption isotherm of Nd^{3+} and Sr^{2+} adsorbed by TTHA•Li-Al LDH.

Fig. 16 Experimental adsorption isotherm for Nd^{3+} and Sr^{2+} adsorbed by TTHA•Li-Al LDH, plotted according to the Langmuir equation (Eq. (10)).

Table captions

Table 1

Chemical compositions of NO_3•Li−Al and TTHA•Li−Al LDHs prepared at initial Li/Al molar ratios of 0.5, 1.0, and 4.0.

Table 2

Average particle size and ζ-potentials of NO_3•Li−Al and TTHA•Li−Al LDH prepared at initial Li/Al molar ratios of 4.0.

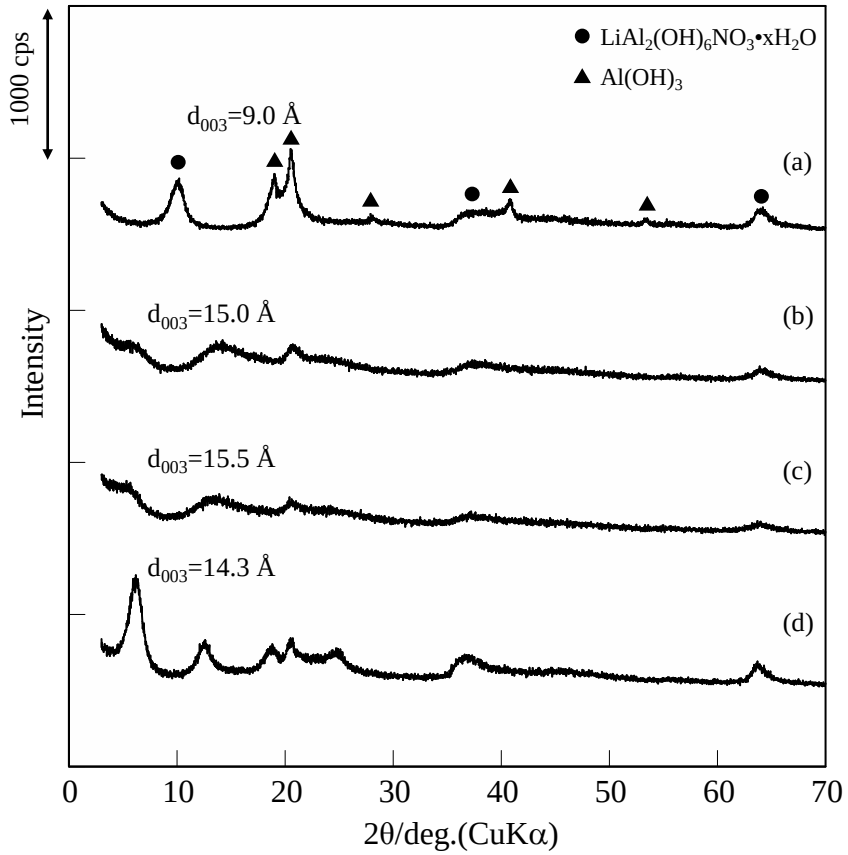

Fig. 1 XRD patterns of (a) NO_3•Li−Al LDH and TTHA•Li−Al LDHs prepared at initial Li/Al molar ratios of (b) 0.5, (c) 1.0, and (d) 4.0.

Table 1 Chemical compositions of NO_3•Li−Al and TTHA•Li−Al LDHs prepared at initial Li/Al molar ratios of 0.5, 1.0, and 4.0.

	Initial Li/Al molar ratio	wt%			molar ratio	
		Li	Al	TTHA	Li/Al	TTHA/Li
NO_3•Li−Al LDH	4.0	1.8	24.0	—	0.3	—
TTHA•Li−Al LDH	0.5	1.7	21.6	33.5	0.3	0.27
	1.0	1.5	19.2	35.4	0.3	0.33
	4.0	3.4	19.6	33.2	0.7	0.14

(a)

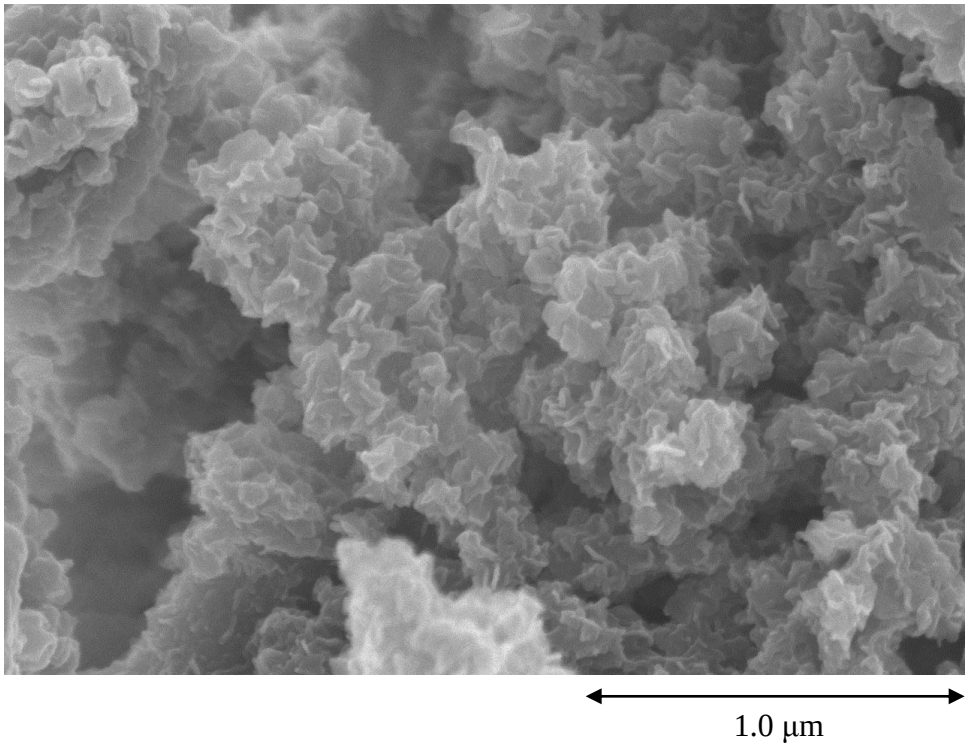

(b)

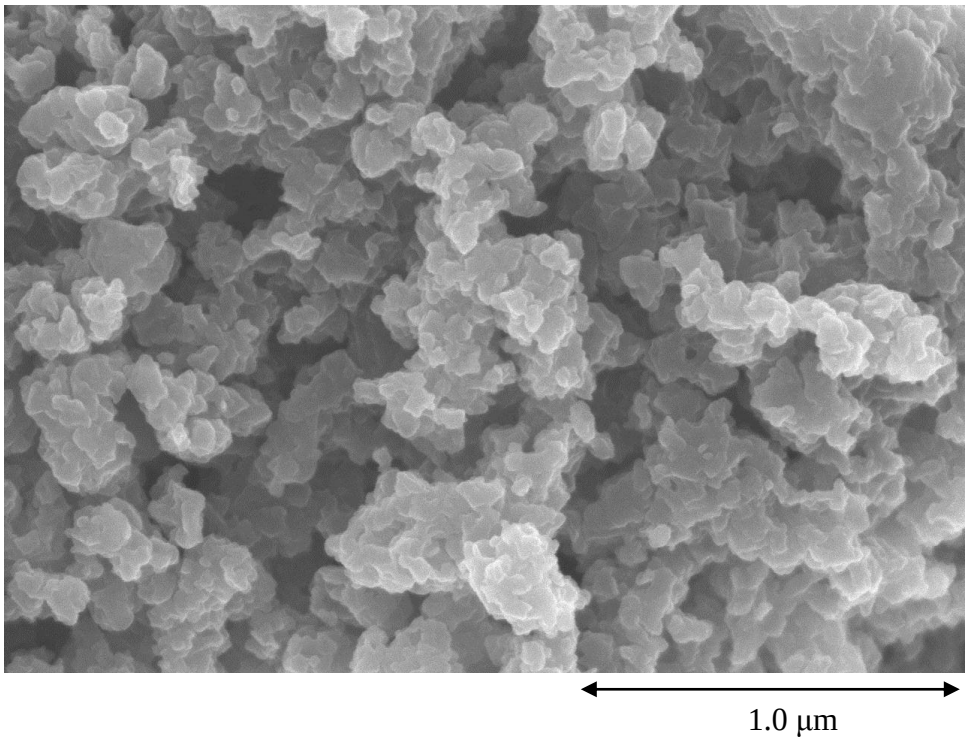

Fig. 2 SEM images of (a) NO_3•Li−Al LDH and (b) TTHA•Li−Al LDH prepared at initial Li/Al molar ratios of 4.0.

Table 2 Average particle size and ζ-potentials of NO_3•Li−Al and TTHA•Li−Al LDH prepared at initial Li/Al molar ratios of 4.0.

	Initial Li/Al molar ratio	Average particle size / nm	ζ-potential / mV
NO_3•Li−Al LDH	4.0	610	+4.88
TTHA•Li−Al LDH	4.0	3023	+4.50

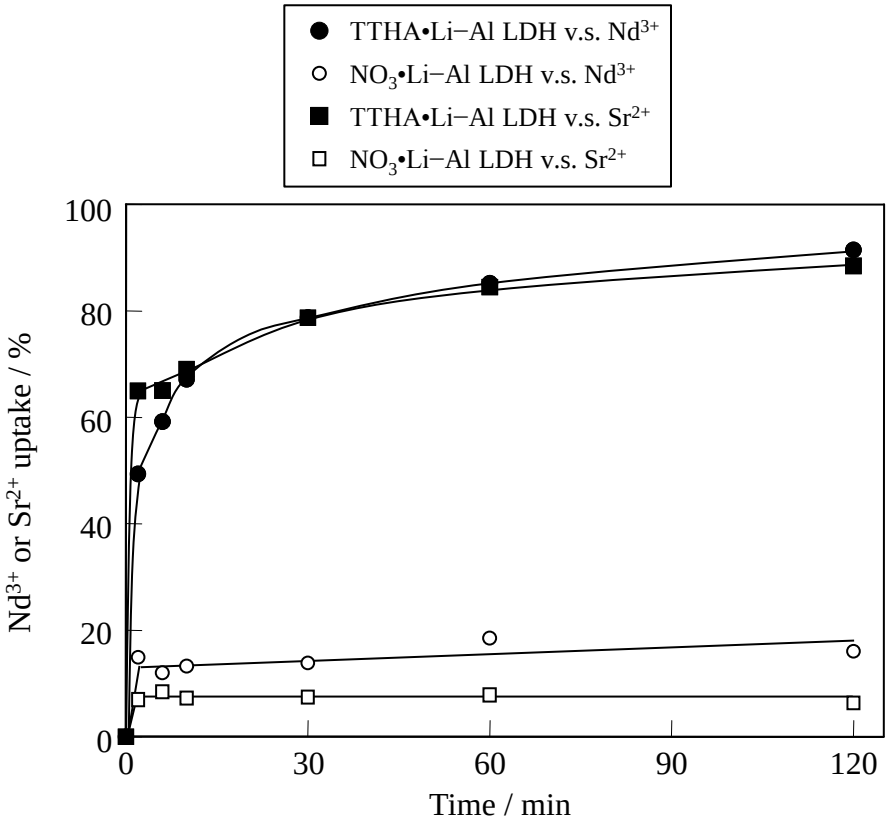

Fig. 3 Variation in Nd^{3+} or Sr^{2+} uptake over time during the suspension of TTHA•Li−Al LDH or NO_3•Li−Al LDH in $Nd(NO_3)_3$ or $Sr(NO_3)_2$ solutions.

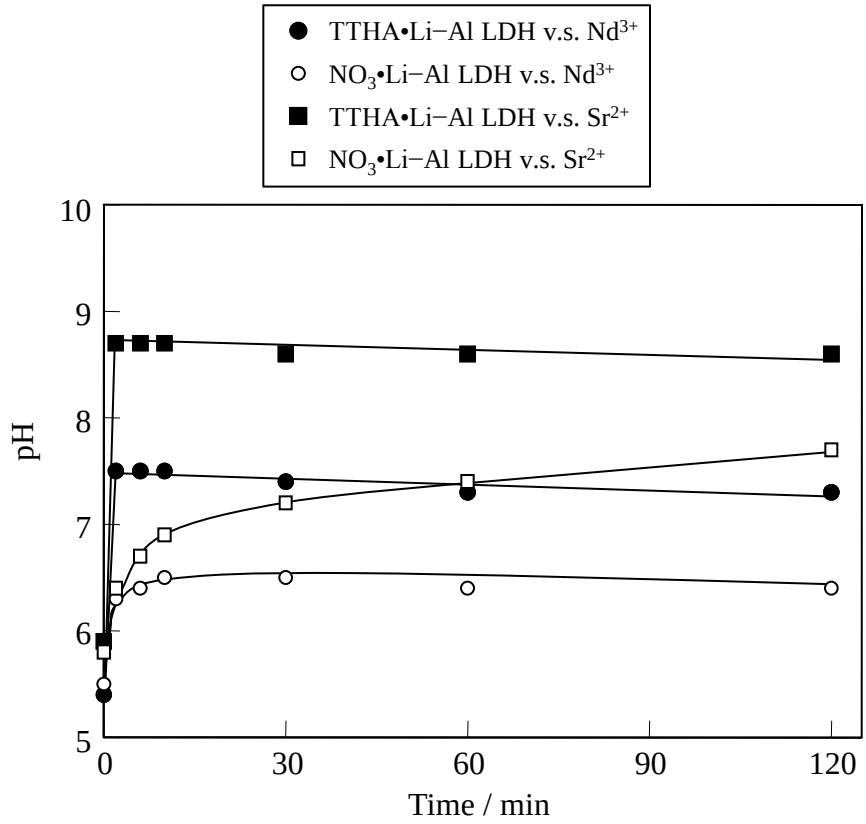

Fig. 4 Variation in pH after Nd^{3+} or Sr^{2+} uptake with time during the suspension of TTHA•Li−Al LDH or NO_3•Li−Al LDH in $Nd(NO_3)_3$ or $Sr(NO_3)_2$ solutions.

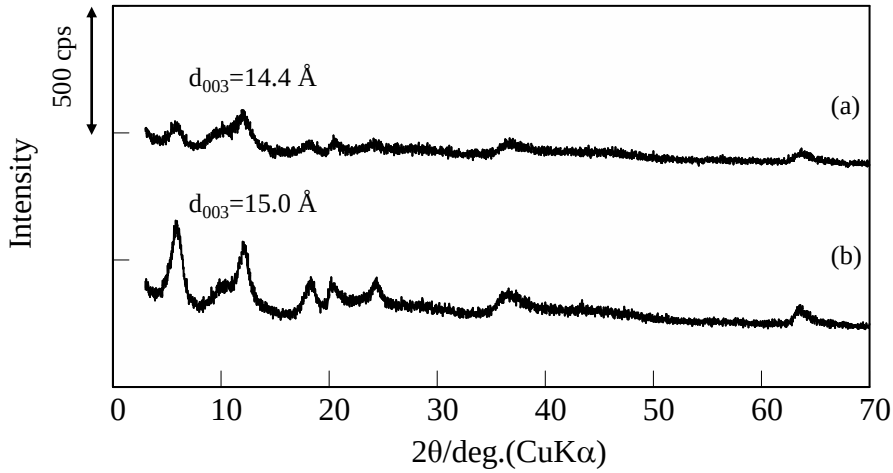

Fig. 5 XRD patterns of the products obtained from the suspension of TTHA•Li−Al LDH in (a) $Nd(NO_3)_3$ and (b) $Sr(NO_3)_2$ solutions in 120 min.

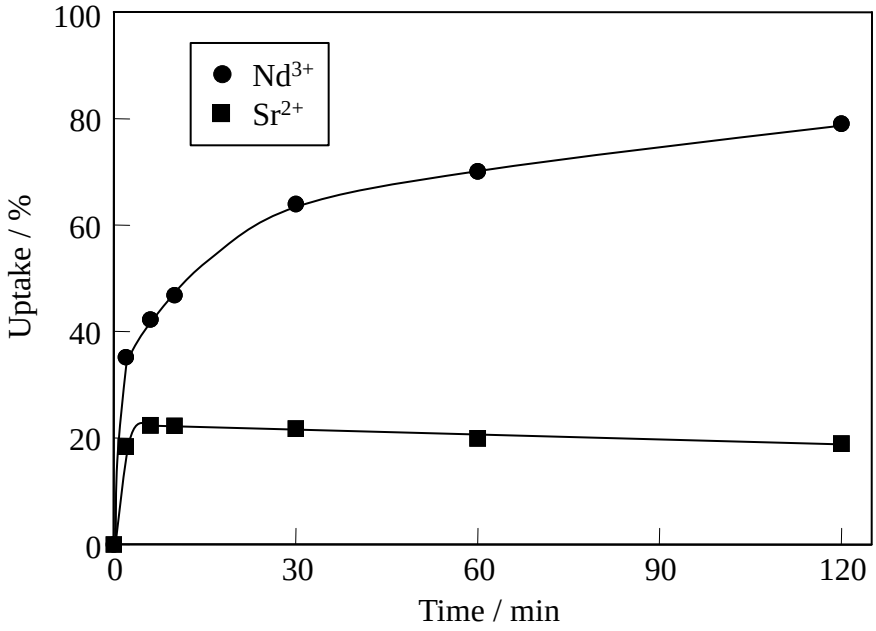

Fig. 6 Variations in Nd^{3+} and Sr^{2+} uptake with time during the suspension of TTHA•Li−Al LDH in 1:1 mixed nitrate solution of Nd^{3+} and Sr^{2+}.

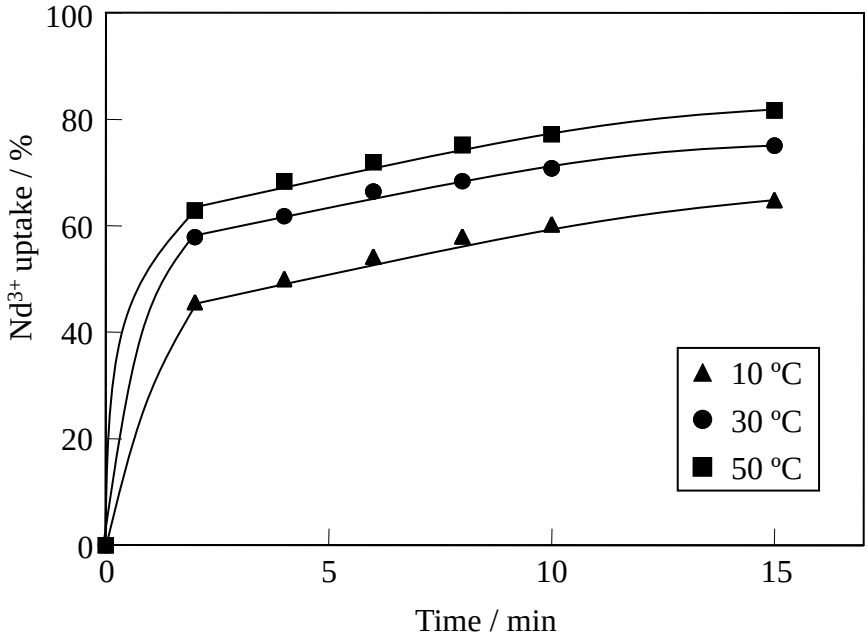

Fig. 7 Effect of temperature on the degree of Nd^{3+} uptake by the suspension of TTHA•Li-Al LDH in $Nd(NO_3)_3$ solution.

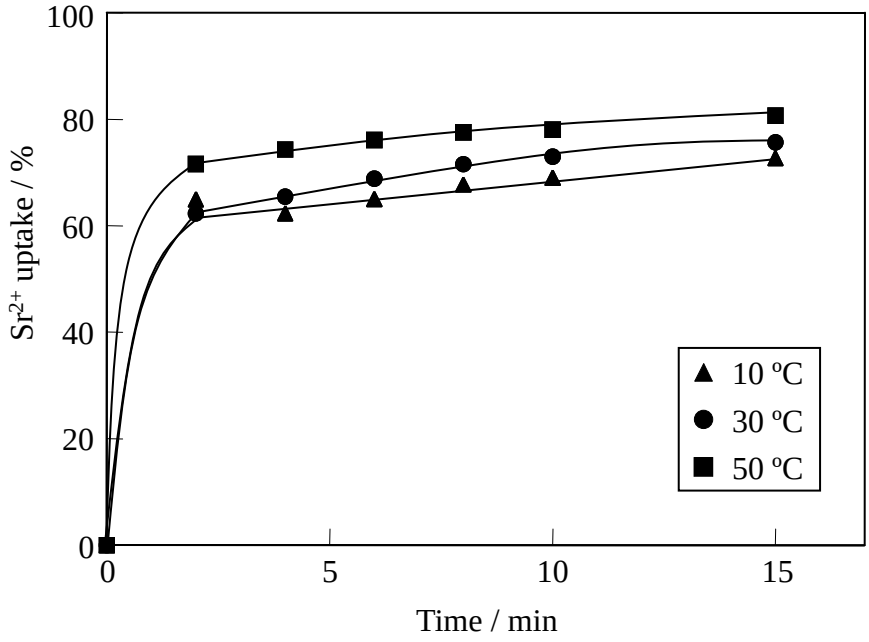

Fig. 8 Effect of temperature on the degree of Sr^{2+} uptake by the suspension of TTHA•Li-Al LDH in $Sr(NO_3)_2$ solution.

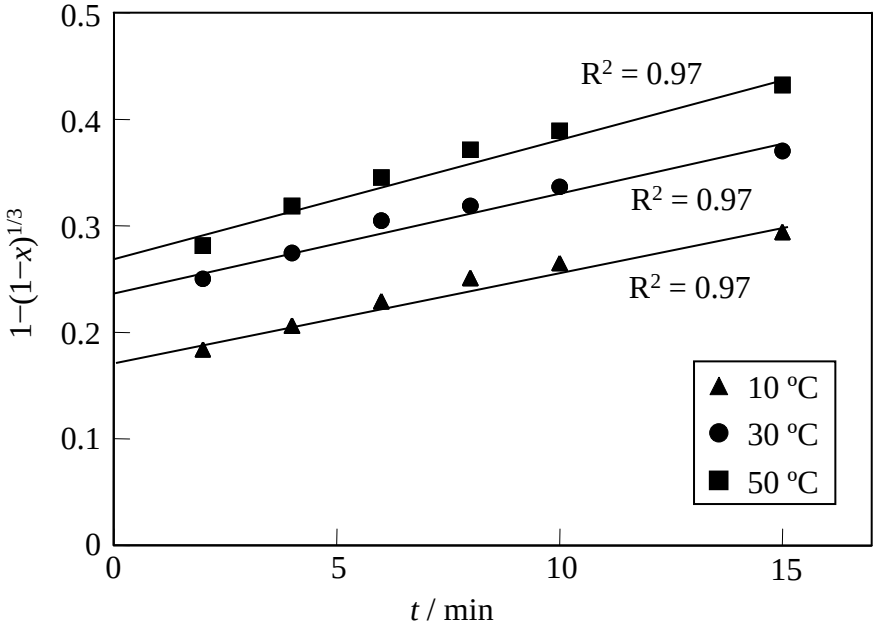

Fig. 9 Experimental data for the uptake of Nd^{3+} by TTHA•Li-Al LDH, plotted according to the equation describing surface chemical reaction control (Eq. (7)).

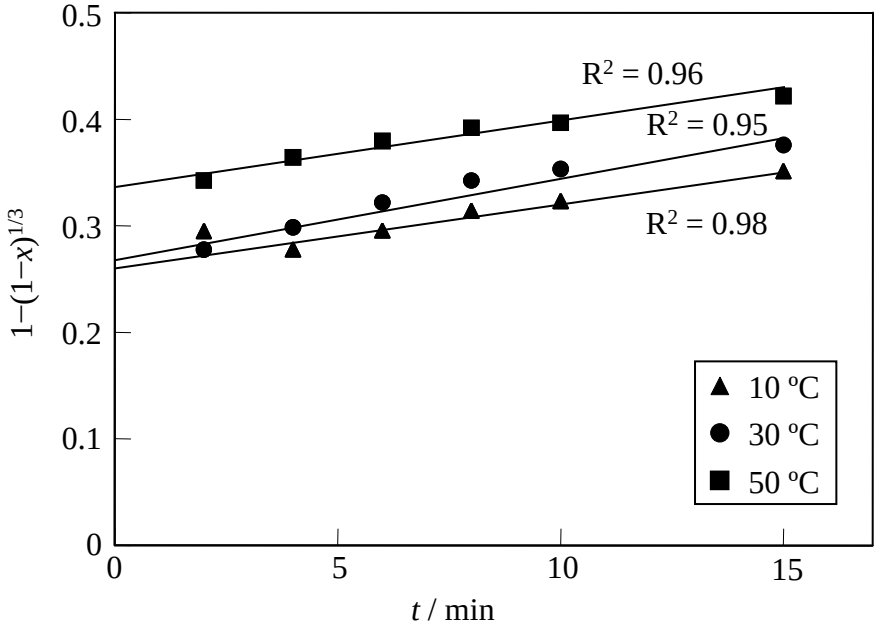

Fig. 10 Experimental data for the uptake of Sr^{2+} by TTHA•Li-Al LDH, plotted according to the equation describing surface chemical reaction control (Eq. (7)).

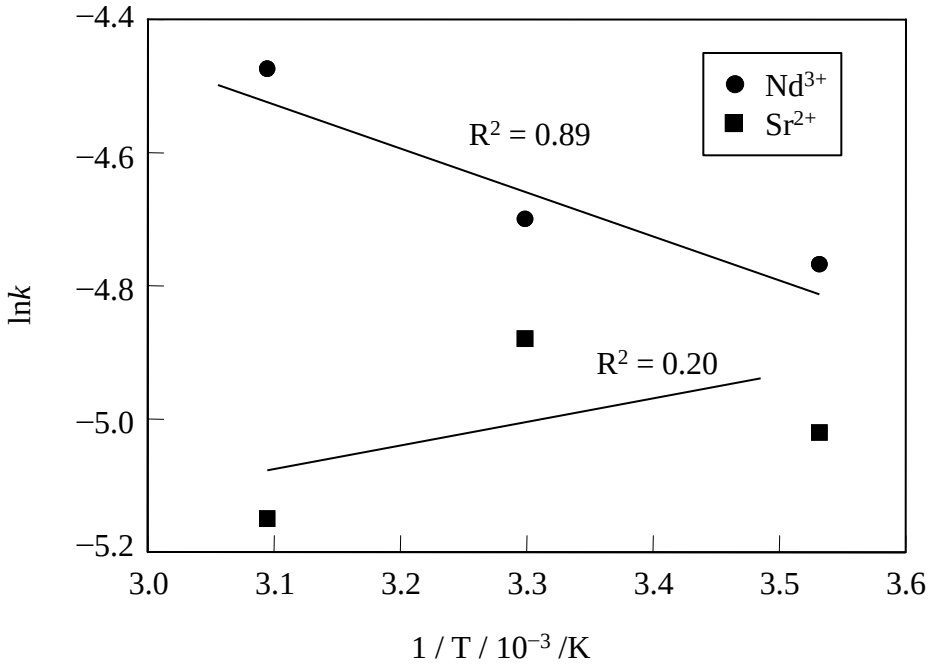

Fig. 11 Arrhenius plot of the apparent rate constants for surface chemical reaction control during the uptake of Nd^{3+} and Sr^{2+} by TTHA•Li-Al LDH.

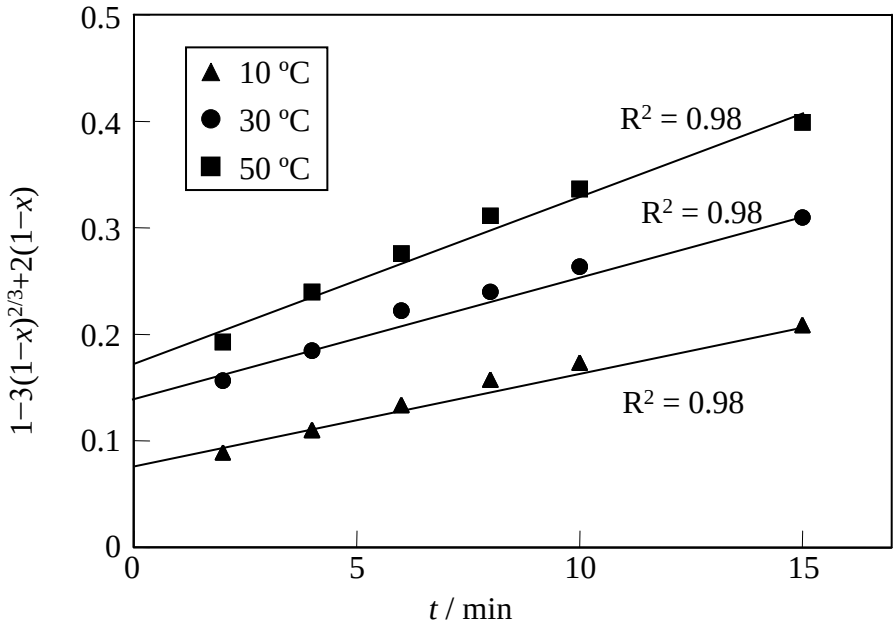

Fig. 12 Experimental data for the uptake of Nd^{3+} by TTHA•Li-Al LDH, plotted according to the equation describing mass transfer control (Eq. (8)).

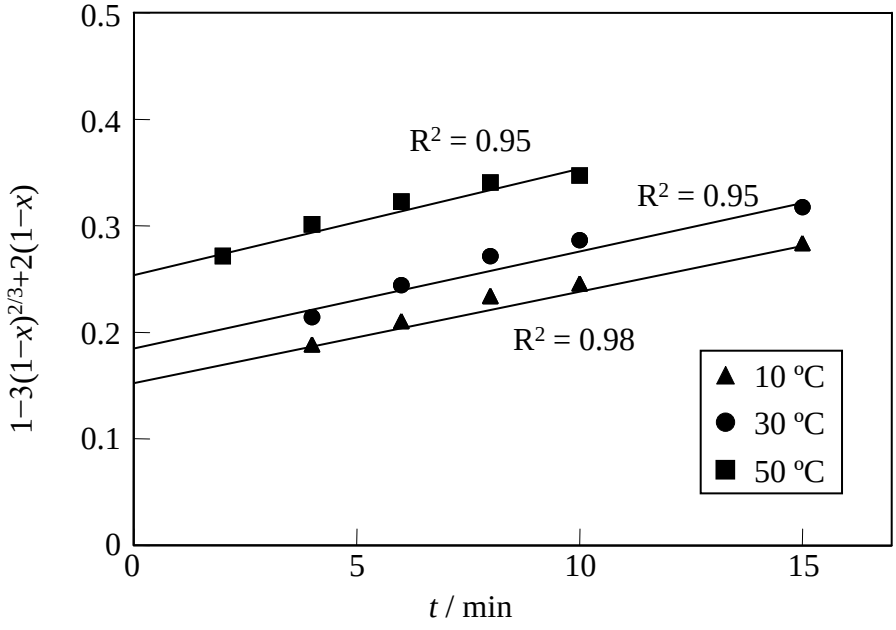

Fig. 13 Experimental data for the uptake of Sr^{2+} by TTHA•Li-Al LDH, plotted according to the equation describing mass transfer control (Eq. (8)).

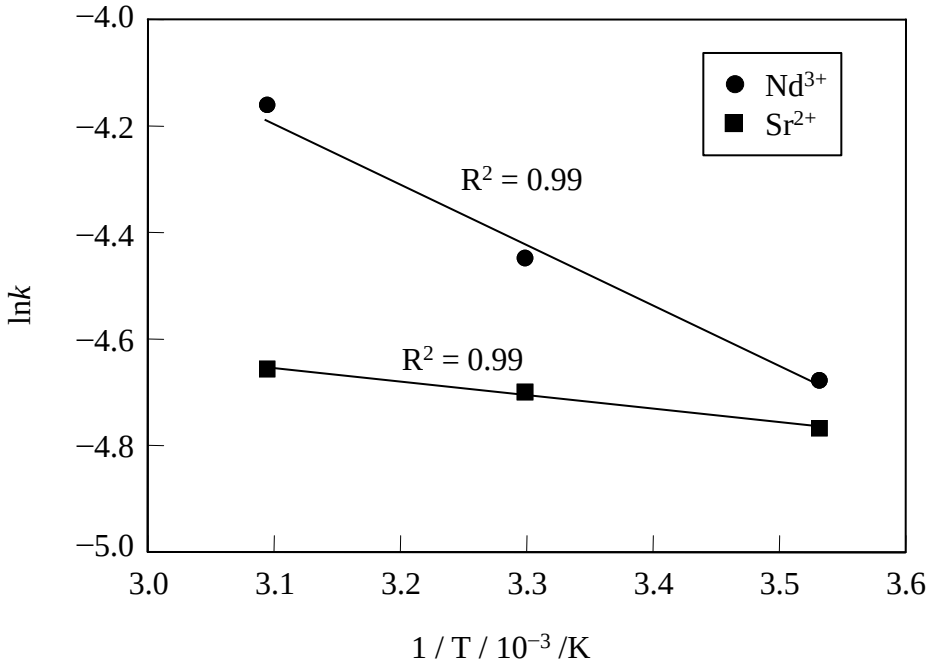

Fig. 14 Arrhenius plot of the apparent rate constants for mass transfer control during the uptake of Nd^{3+} and Sr^{2+} by TTHA•Li-Al LDH.

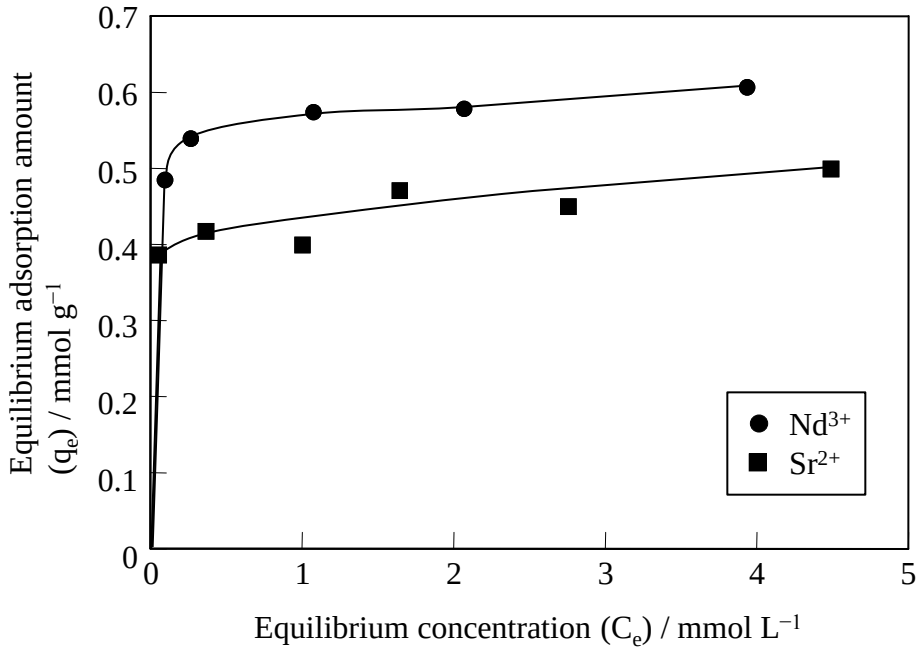

Fig. 15 Adsorption isotherm of Nd^{3+} and Sr^{2+} adsorbed by TTHA•Li-Al LDH.

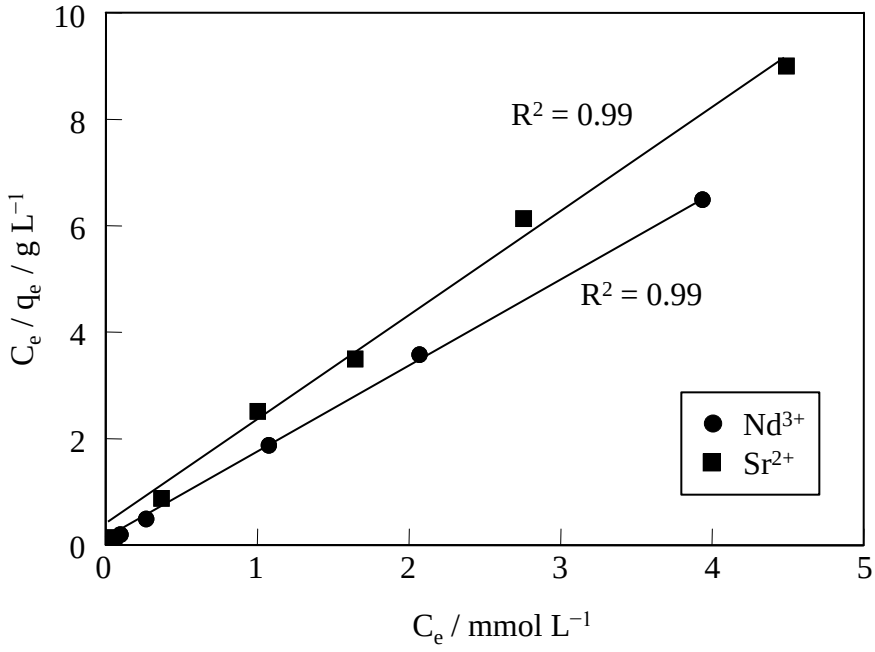

Fig. 16 Experimental adsorption isotherm for Nd^{3+} and Sr^{2+} adsorbed by TTHA•Li-Al LDH, plotted according to the Langmuir equation (Eq. (10)).